

See discussions, stats, and author profiles for this publication at: <https://www.researchgate.net/publication/260817884>

Experimental Evidence Shedding Light on the Origin of the Reduction of Branching of Acrylates in ATRP

ARTICLE in MACROMOLECULES · FEBRUARY 2014

Impact Factor: 5.8 · DOI: 10.1021/ma4025637

CITATIONS

11

READS

50

6 AUTHORS, INCLUDING:



Nicholas Ballard

The University of Warwick

23 PUBLICATIONS 182 CITATIONS

[SEE PROFILE](#)



J. Ignacio Santos

Universidad del País Vasco / Euskal Herriko U...

42 PUBLICATIONS 579 CITATIONS

[SEE PROFILE](#)



Fernando Ruipérez

Universidad del País Vasco / Euskal Herriko U...

52 PUBLICATIONS 417 CITATIONS

[SEE PROFILE](#)



Jose R Leiza

Universidad del País Vasco / Euskal Herriko U...

145 PUBLICATIONS 2,529 CITATIONS

[SEE PROFILE](#)

Experimental Evidence Shedding Light on the Origin of the Reduction of Branching of Acrylates in ATRP

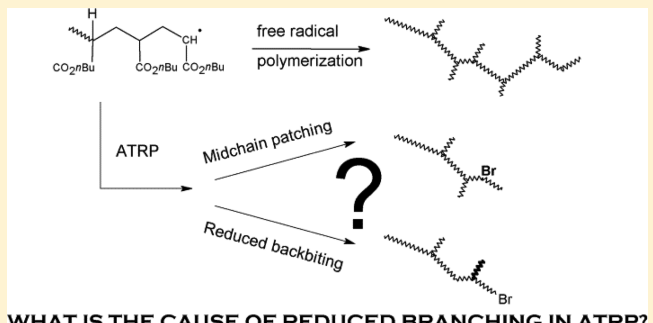
Nicholas Ballard,[†] Maitane Salsamendi,[†] José Ignacio Santos,[‡] Fernando Ruipérez,[†] Jose R. Leiza,[†] and Jose M. Asua^{*,†}

[†]POLYMAT and Grupo de Inginería Química, Dpto. de Química Aplicada, University of the Basque Country UPV/EHU, Joxe Mari Korta Zentroa, Tolosa Etorbidea 72, 20018, Donostia/San Sebastian, Spain

[‡]NMR Facility, SGiker, University of the Basque Country UPV/EHU, Joxe Mari Korta Zentroa, Tolosa Hiribidea 72, 20018 Donostia-San Sebastián, Spain

Supporting Information

ABSTRACT: Intramolecular chain transfer to polymer and subsequent propagation of tertiary radicals cause extensive branching in radical polymerization of acrylic monomers. Studies in the literature have shown that under controlled radical polymerization conditions the extent of branching is significantly reduced. There are two competing theories to explain this effect. In one, the cause of reduced branching is attributed to a reduction in the number of backbiting events, and in the other that has been specifically applied to atom-transfer radical polymerization (ATRP), the cause is due to trapping of the tertiary radical by a fast deactivation step. In this article we show that trapping of the tertiary radical is not the cause for the reduction in branching fraction. This is shown by the absence of the corresponding patched midchain bromide structure as revealed by quantitative ¹³C NMR and by the ability to chain extend from a poly(butyl acrylate-*co*-butyl 2-bromoacrylate) copolymer by ATRP. These results are complemented by quantum mechanical computations.



WHAT IS THE CAUSE OF REDUCED BRANCHING IN ATRP?

INTRODUCTION

Chain transfer to polymer has a great impact on the kinetics of free radical polymerization of acrylates as well as on the microstructure and properties of these materials.^{1–14} Chain transfer to polymer can occur via either an intramolecular process (backbiting), leading to short branches, or an intermolecular process, leading to long branches (Scheme 1). Experimentally, intramolecular chain transfer to polymer has been shown to be the dominant mechanism in the formation of branching points, both in solution and in dispersed phase systems.^{2,6,15,16} The intramolecular process tends to proceed via the energetically favorable, six-membered ring structure resulting in a 1,5 hydrogen transfer leading to a midchain radical.^{17,18} The existence of the midchain radical and its slow propagation rate has been confirmed by EPR and has highlighted the importance of secondary reactions, such as β -scission, that can occur due to the prolonged lifetime of the midchain radical.^{6,13,19–23} For polymerizations carried out at moderate temperatures (<100 °C) propagation of the tertiary radical is the most likely fate of the midchain radical leading to the formation of quaternary carbons and a fingerprint of this process can be detected by ¹³C NMR.^{1–3,24–27}

It was soon recognized that as branching mainly results from the competition between a first-order process (backbiting) and a second-order process (propagation), each of them with different activation energies, the extent of branching depends

on the polymerization conditions and increases with temperature and as the concentration of monomer decreases.^{1,2,7,14,26,28} More recently, it has been reported that branching is affected by other process variables such as the type of solvent,^{29,30} the presence of high concentrations of chain transfer agents,^{21,31,32} and pulse time in pulsed laser polymerizations.^{12,33}

In addition, substantial evidence in the literature shows that in controlled radical polymerizations the amount of branching is significantly reduced, though the exact cause of this has not been conclusively resolved. An initial study by Ahmad et al. suggested that the main cause for this effect was the difference between concentrations of short chain and long chain radicals in controlled and free radical polymerizations that, due to the chain length dependent rate coefficients, affected the branching level.³⁴ However, Reyes and Asua³⁵ and Konkolewicz et al.³⁶ have since shown by simulation that there is a minimal influence of chain length dependent rate coefficients on branching density. These two groups offered two different explanations for the decrease of branching in CRP. Reyes and Asua³⁵ proposed that the decrease was due to a reduction in the number of backbiting reactions because the time between

Received: December 16, 2013

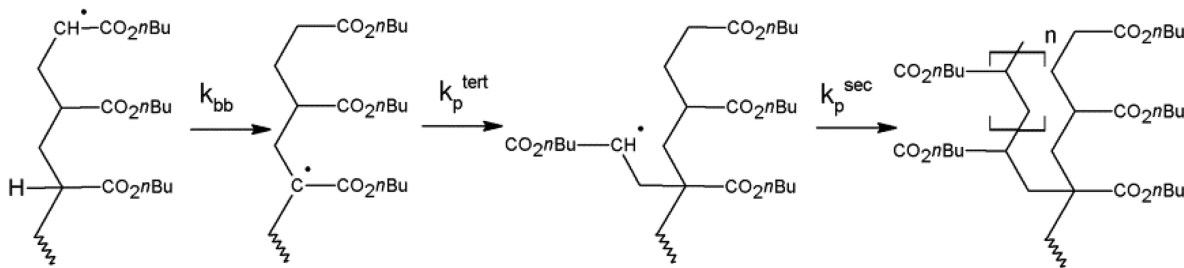
Revised: January 16, 2014

Published: January 27, 2014

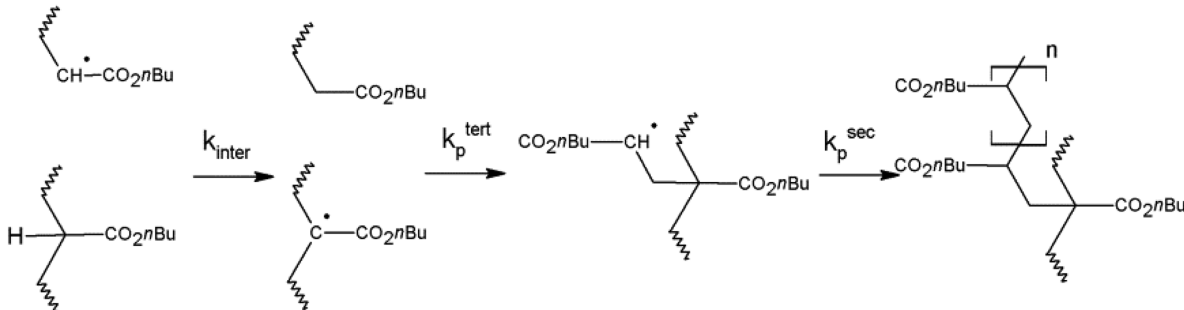
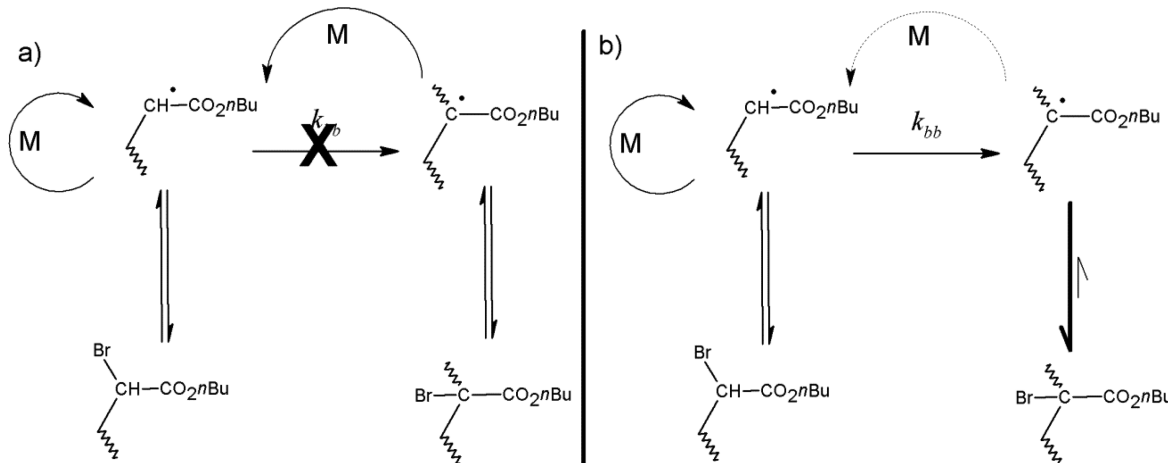


Scheme 1. Processes by Which Chain Transfer to Polymer Can Occur in Free Radical Polymerization of Acrylic Monomers

Intramolecular chain transfer to polymer



Intermolecular chain transfer to polymer

Scheme 2. Conflicting Theories on the Origin of Reduced Branching in ATRP of Poly(butyl acrylate)^a

^a(a) Probability of backbiting is reduced due to short transient lifetime resulting in a lower rate of production of the midchain radical.³⁵ (b) Competitive processes in the ATRP process result in a buildup of the midchain bromide as tertiary radical reacts slowly to regenerate the secondary radical species.³⁶

activation and deactivation of the radicals is of the same order of magnitude or shorter than the time required for the conformation change necessary for intramolecular hydrogen atom transfer. Using a stochastic model and arbitrary distributions for the reaction times, they predicted that, in agreement with the experimental data, C_q decreases when the concentration of the control agent increased. Conversely, in a computational study of the atom-transfer radical polymerization of butyl acrylate, Konkolewicz et al.³⁶ concluded that the number of backbiting events was not altered, but rather that the midchain radical formed suffered a relatively fast and virtually irreversible deactivation. Scheme 2 summarizes these conflicting theories. This scheme shows that the presence of bromide atoms on quaternary carbons should leave a fingerprint based

on the theory proposed by Konkolewicz et al.³⁶ Therefore, in this article we have conducted experiments to conclusively determine whether buildup of bromide capped midchain radicals is responsible for the reduction in branching in ATRP. In order to investigate this, we have synthesized a model copolymer of poly(butyl acrylate-*co*-butyl 2-bromoacrylate) and show that the signals attributed to the capped bromine species do not appear in the NMR spectra of poly(butyl acrylate) synthesized by ATRP. In addition, we demonstrate efficient growth of branches from macroinitiators containing tertiary bromides that indicates that deactivation of tertiary radicals is not irreversible. This is further supported by *ab initio* calculations that demonstrate that the energy for the activation

of the bromide capped midchain radical is less than for secondary radicals.

EXPERIMENTAL SECTION

Materials. Butyl acrylate (Quimidroga, technical grade) was filtered through a basic alumina column before use. Azobis(isobutyronitrile) (Aldrich, 98%), bromine (Aldrich, reagent grade), potassium carbonate (Aldrich, 99%), copper(I) bromide (Aldrich, 98%), copper(II) bromide (Aldrich, 99%), propylamine (Aldrich, 98%), and 2-pyridinecarboxaldehyde (Aldrich, 99%) were used as received. All other solvents were purchased from Scharlab and were used without purification.

Methods. NMR spectra were recorded at 25 °C on a Bruker AVANCE 500 MHz equipped with a z-gradient double resonance probe. 1D ¹H spectra were acquired by use of 32K data points which were zero-filled to 64K data points prior to Fourier transformation. 1D ¹³C spectra were recorded at a ¹³C Larmor frequency of 125.77 MHz. The spectra were recorded using 20 000 transients. Quantitative ¹³C spectra were recorded using single pulse excitation, using a 5.5 μs 90° pulse, inverse gated waltz16 decoupling to avoid NOE effects and a relaxation delay of 10 s. Apodization was achieved using an exponential window function equivalent to a line width of 10 Hz. 1D ¹³C DEPT-135 spectra were acquired for 16 000 transients using single pulse excitation, using a 5.5 μs 90° pulse, inverse gated waltz16 decoupling to avoid NOE effects, and a relaxation delay of 10 s. Apodization was achieved using an exponential window function equivalent to a line width of 3 Hz. 2D NMR spectra were recorded in HSQC and HMBC experiments. The spectral widths for the HSQC experiment were 5000 and 25 000 Hz for the ¹H and the ¹³C dimensions, respectively. The number of collected complex points was 2048 for the ¹H dimension with a recycle delay of 5 s. The number of transients was 64 and 256 time increments were recorded in the ¹³C dimension. The ¹J_{CH} used was 140 Hz. The J-coupling evolution delay was set to 3.2 ms. The squared cosine-bell apodization function was applied in both dimensions. Prior to Fourier transformation, the data matrices were zero-filled to 1024 points in the ¹³C dimension. For the HMBC experiment the spectral widths were 2000 and 32 000 Hz for the ¹H and the ¹³C dimensions, respectively. The ¹J_{CH} used was 145 Hz, and ¹J_{CH} was 10 Hz. The J-coupling evolution delay was set to 3.4 and 50 ms. The number of transients was 1024, and 16 time increments were recorded in the ¹³C dimension. The spectrum was processed with a cosine window function in each dimension and one level of zero filling in F1 and is presented in magnitude mode.

The branching density of the polymers were calculated from quantitative ¹³C spectra from the ratio of the integral of the quaternary carbon peak (45–49 ppm) and the methyl group of the butyl ester (11–14 ppm).³²

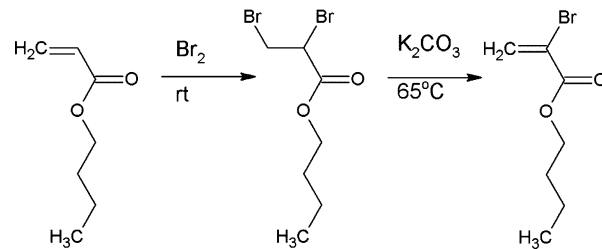
Molecular weight distributions were measured by size exclusion chromatography (SEC). Samples taken from ATRP experiments for molecular weight analysis were first diluted with THF and filtered through a short column of neutral alumina before being further diluted to a concentration of approximately 1 mg mL⁻¹ and filtered through a 0.45 μm nylon filter. Samples from bulk polymerization experiments were diluted with THF and filtered through the nylon filter prior to injection into the SEC. The SEC set up consisted of a pump (LC-20A, Shimadzu), an autosampler (Waters 717), a differential refractometer (Waters 2410), and three columns in series (Styragel HR2, HR4, and HR6 with pore sizes ranging from 10² to 10⁶ Å). Chromatograms were obtained at 35 °C using a flow rate of 1 mL min⁻¹. The equipment was calibrated using narrow polystyrene standards ranging from 595 to 3.95 × 10⁶ Da (fifth-order universal calibration). The resulting molecular weight distribution was recalibrated using Mark–Houwink parameters of 12.2 × 10⁻⁵ dL g⁻¹, α = 0.70 for poly(butyl acrylate) and 15.2 × 10⁻⁵ dL g⁻¹, α = 0.70 for polystyrene.^{37,38}

Synthesis of *N*-(*n*-Propyl)-2-pyridylmethanimine. *N*-(*n*-Propyl)-2-pyridylmethanimine was synthesized according to the report by Haddleton et al.³⁹ Briefly, to a stirred solution of pyridine-2-carboxaldehyde (5.35 g, 0.05 mol) in diethyl ether (5 g) on ice was added *n*-propylamine (3.54 g, 0.06 mol) dropwise. Sodium sulfate (1

g) was added, and the reaction was left at room temperature for 4 h. The suspension was filtered, and solvent was removed by rotary evaporation to yield golden oil (7.14 g, 96.5% yield). ¹H NMR (CDCl₃): δ 8.51 (m, 1H), 8.26 (s, 1H), 7.84 (m, 1H), 7.60 (m, 1H), 7.17 (m, 1H), 3.52 (t, 2H), 1.63 (m, 2H), 0.84 (t, 3H). ¹³C NMR (CDCl₃): δ 161.4, 154.3, 149.0, 136.1, 124.2, 120.8, 63.9, 23.5, 11.5.

Synthesis of *n*-Butyl 2-Bromoacrylate. Butyl 2-bromoacrylate was synthesized in a two-step method according to Scheme 3 using a

Scheme 3. Synthesis of Butyl 2-Bromoacrylate



previously described method.⁴⁰ To butyl acrylate (30 g) in carbon tetrachloride (80 mL) was added bromine (37.5 g) dropwise at room temperature. The reaction mixture was left overnight, and volatiles were removed by rotary evaporation to yield 2,3-dibromopropionate as a clear, faintly yellow oil (65 g, 96% yield). ¹H NMR (CDCl₃): δ 4.44 (1H, dd), 4.26 (2H, t), 3.94 (1H, t), 3.69 (1H, dd), 1.69 (2H, t), 1.45 (2H, q), 0.97 (3H, t). ¹³C NMR (CDCl₃): δ 167.5, 66.8, 41.1, 30.3, 29.7, 18.9, 13.6.

To 2,3-dibromopropionate (64.5 g) in acetonitrile (180 g) was added hydroquinone (100 mg) and potassium carbonate (70 g). The reaction was heated to 65 °C and left overnight. The suspension was cooled and filtered. The solvent was removed from the filtrate, and the residue dissolved in chloroform. The organic solution was washed with water, then dried with anhydrous sodium sulfate, and filtered, and the solvent was removed to yield a clear oil (34.6 g, 75% yield). ¹H NMR (CDCl₃): δ 6.96 (1H, s), 6.27 (1H, s), 4.24 (2H, t), 1.70 (2H, q), 1.43 (2H, t), 0.97 (3H, t). ¹³C NMR (CDCl₃): δ 162.2, 130.6, 121.9, 66.8, 30.7, 19.3, 13.9.

Bulk Polymerization of Poly(*n*-butyl acrylate). Bulk polymerization of butyl acrylate was carried out in a two-neck round-bottomed flask under a nitrogen atmosphere. AIBN (5 mg) was dissolved in butyl acrylate (1 g), and nitrogen was bubbled through for 10 min. The flask was sealed and heated to 90 °C for 4 h. After polymerization the sample was dried in air for 24 h to remove excess monomer. No precipitation was performed in order to avoid any fractionation of the polymer.

Bulk Polymerization of Poly(*n*-butyl 2-bromoacrylate). Bulk polymerization of butyl 2-bromoacrylate was carried out in a two-neck round-bottomed flask fitted with a reflux condenser. AIBN (5 mg) was dissolved in *n*-butyl 2-bromoacrylate (1 g) and nitrogen bubbled through for 10 min. The flask was sealed and heated to 70 °C for 4 h. After polymerization the sample was dried in air for 24 h to remove excess monomer.

Bulk Copolymerization of Poly(*n*-butyl acrylate-*co*-*n*-butyl 2-bromoacrylate). Copolymerizations were conducted in sealed vials. AIBN (2.5 mg) was dissolved in the reaction mixture containing varying quantities of butyl acrylate and *n*-butyl 2-bromoacrylate (total 0.5 g), and nitrogen was bubbled through the solution for 1 min. The vials were sealed and placed in a water bath at 70 °C for 4 h. For analysis of reactivity ratios the polymerization mixture was prepared in the same way, but polymerizations were conducted only to low conversion (<10%) by leaving to react for 10 min and then placing the vials in ice. When the reaction mixture had cooled sufficiently, the polymers were precipitated in a 90:10 wt/wt methanol–water mixture, filtered, and placed under vacuum for 24 h to remove volatile components.

Reactivity ratios were determined from low conversion copolymer compositions by ¹H NMR, comparing the backbone CH of the butyl acrylate part at 2.3 ppm to the signal from the terminal methyl protons

of the butyl chain, of varying monomer feed compositions. The terminal model was used, and the data were fit using a nonlinear least-squares method based on the minimization of the sum of least-squares space introduced by van Herk.⁴¹ The data were weighted on the assumption of a constant relative error in the copolymer composition, and the joint confidence interval was determined by the F-test method.

ATRP Polymerization of Butyl Acrylate. Copper(II) bromide (17 mg, 0.076 mmol), copper(I) bromide (100 mg, 0.69 mmol), butyl acrylate (10 g, 0.078 mol), and *N*-(*n*-propyl)-2-pyridylmethanimine (347 mg, 2.34 mmol) were placed in a round-bottomed flask and bubbled with nitrogen for 30 min. The reaction solution was heated to 90 °C, and the initiator, methyl bromoisobutyrate (100 μL, 0.77 mmol), was added by syringe. Samples were taken during the course of reaction to determine conversion by gravimetry and molecular weight. Following the reaction the mixture was diluted with toluene and filtered through an alumina column and subsequently dried in air for 24 h followed by drying under vacuum for 24 h.

ATRP Chain Extension. The macroinitiator was synthesized by bulk copolymerization of butyl acrylate and butyl 2-bromoacrylate. AIBN (10 mg) and octylthiol (60 mg) were dissolved in a mixture of butyl acrylate (4.75 g) and butyl 2-bromoacrylate (0.25 g). The reaction mixture was bubbled with nitrogen and then heated to 70 °C for 45 min. The polymer was dissolved in toluene, then precipitated in methanol, collected by filtration, and dried under vacuum overnight. Final polymer conversion measured by gravimetry was 0.85. $M_n = 11\,700 \text{ g mol}^{-1}$; PDI = 2.2.

2.5 g of the copolymer synthesized above (containing on average 3 mol % butyl 2-bromoacrylate corresponding to a bromide content of 0.6 mmol) was dissolved in 4.65 g of xylene and added to butyl acrylate (4.8 g, 0.0375 mol), *N,N,N',N',N'*-pentamethyldiethylenetriamine (70 μL, 0.33 mmol), copper(I) bromide (40 mg, 0.28 mmol), and copper(II) bromide (2.2 mg, 0.01 mmol). The mixture was degassed by three freeze–pump–thaw cycles and then heated at 80 °C. After 4 h the reaction mixture was cooled on ice, diluted with xylene, and filtered through a short alumina column. The polymer was precipitated in cold MeOH/H₂O (90:10 wt/wt), collected by decanting the liquid from the polymer phase, and drying the polymer overnight under vacuum.

Quantum Mechanical Calculations. Density functional calculations (DFT) have been performed using the Gaussian 09⁴² suite of programs employing the M06-2X functional⁴³ in conjunction with the correlation-consistent valence triple- ζ basis set (cc-pVTZ) developed by Dunning and co-workers^{44–46} for all atoms. Geometry optimizations were carried out in gas phase and in acetonitrile by means of the polarizable continuum model (PCM).^{47–50}

To confirm that the optimized structures were minima in the potential energy surfaces, frequency calculations were done at the same level of theory. All structures showed real frequencies for all the normal modes of vibration. The frequencies were then used to evaluate the zero-point vibrational energy (ZPVE) and the thermal ($T = 298 \text{ K}$) vibrational corrections to the Gibbs free energy in the harmonic oscillator approximation.

RESULTS

The principal objective of this study was to determine whether permanent patching of the midchain radical by a bromine atom in ATRP could be responsible for the reduced level of branching observed compared to free radical polymerization of butyl acrylate. To begin, we conducted a polymerization by ATRP and one by conventional free radical polymerization and attempted to determine whether any additional peaks were observable in the spectra of those produced by ATRP and whether they could be attributed to the patched structure. The reaction performed by ATRP showed typical characteristics of a living polymerization with increasing molecular weight with conversion and linear first-order rate plot for the reaction (see Figures S1 and S2 in the Supporting Information). Table 1 shows the molecular weight and the degree of branching for the

Table 1. Difference in Extent of Branching in Free Radical and ATRP Polymerization of Poly(butyl acrylate) Conducted at 90 °C

	X	M_w (kDa)	PDI	DB ^a (%)
free radical	0.86	140	18	3.26 ± 0.22
ATRP	0.94	21.1	1.33	1.08 ± 0.02

^aError bar estimated based on the signal-to-noise ratio of the C_q signal in the ¹³C NMR spectra.²⁷

two samples in which it can clearly be seen that the degree of branching is lower in the sample produced by ATRP in accordance with previous reports. As may be expected, the PDI was lower in the case of the ATRP polymerization while the number molecular weights are similar.

The ¹³C NMR spectra of the two samples were largely identical as can be expected. The assigned spectra can be seen in Figure 1. The main differences are solely in the end groups

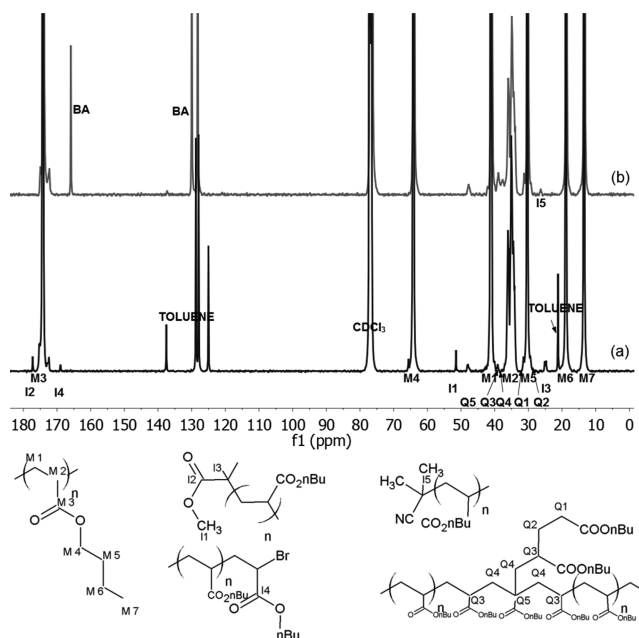


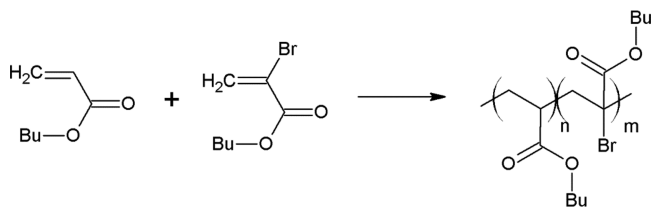
Figure 1. NMR spectra of poly(butyl acrylate) by (a) ATRP and (b) free radical polymerization and the assigned positions.

that can be seen for the ATRP reaction and the slight reduction in signals that arise due to branching. The assignments of the end groups are in agreement with the DEPT-135 spectra (see Figure S4) and ppm shifts predicted by a chemical shift substituent increment scheme for alkanes and the integral values of the quantitative ¹³C spectra. The peak at 65.5 ppm that appears as a shoulder to the main OCH₂ signal is almost certainly due to the OCH₂ located at the bromide capped end group based on the fact that it is reduced when the amount of initiator is lowered, which lowers the expected number of polymer chains and increases their molecular weight; therefore, the ratio of end group peaks to monomer units should also decrease. In addition, the peak did not shift when methyl 2-propionate was used as initiator instead of methyl bromoisobutyrate (see Figure S8), and previous reports on polymerization using high quantities of CBr₄ also showed this peak.³² There are several signals which are difficult to assign with confidence due to the extent of overlapping with other carbons of much greater signal intensity, most notably either side of the

COOnBu carbonyl carbon at 174 ppm and much smaller signals either side of the carbon related to the CH in the backbone. The peaks in the carbonyl region presumably arise from carbonyls near to the quaternary carbon because they appear to be relative to the integral of the quaternary carbon, but there is not sufficient resolution of the peaks to definitively assign them to a single structure.

The quantitative analysis of the two carbon spectra showed no new peaks and thus seemed to conflict with the idea that the quaternary radical is patched, forming a midchain bromide, during the ATRP reaction. However, in order to confirm that there was no possibility of overlap of the peaks corresponding to this structure with that of poly(butyl acrylate), we synthesized a poly(butyl acrylate) polymer with a bromide in the backbone at the same position as it would occur in the "patched" structure. In order to realize this, we copolymerized butyl acrylate with varying amounts of butyl 2-bromoacrylate by bulk free radical copolymerization using AIBN as thermal initiator (see Scheme 4).

Scheme 4. Synthesis of Poly(butyl acrylate-*co*-butyl 2-bromoacrylate), a Midchain Bromide-Containing Polymer



In order to accurately assign the NMR spectra of the copolymer, we first synthesized the homopolymer of butyl 2-bromoacrylate by bulk free radical polymerization. In all polymerizations containing this monomer a lower reaction temperature (70°C) was used in order to avoid potential side reactions of both the monomer and the resulting polymer and to maintain a low degree of branching that makes changes in branching density easier to detect in later experiments. The ^1H and ^{13}C NMR spectra of the homopolymer and the corresponding assignments are given in Figure 2. There are some notable shifts in both spectra for both carbon and hydrogens that are close to the midchain bromide. The signals arising from backbone hydrogen (BH1) and carbon atoms (B1 and B2) shift to higher ppm in both the ^1H and ^{13}C NMR. The OCH_2 carbon is shifted to higher ppm and the carbonyl peak is at lower ppm than the corresponding poly(butyl acrylate) spectra. These assignments can be verified by HSQC and HMBC spectra that are given in the Supporting Information.

From the assignments of the poly(butyl 2-bromoacrylate) we proceeded to determine whether the signals arising from the midchain bromide can be distinguished from the butyl acrylate signals in samples of poly(butyl acrylate) produced by ATRP. To do this, we copolymerized varying amounts (5–50 wt %) of butyl 2-bromoacrylate with butyl acrylate. In Figure 3 it can be seen that upon increasing the content of butyl 2-bromoacrylate the peak corresponding to the OCH_2 next to a midchain bromide (around 66.5 ppm) visibly increases and can be easily observed at 5 wt % even using low-resolution, nonquantitative NMR techniques. In the hydrogen NMR, the location of the backbone peak changes with varying quantities of butyl 2-bromoacrylate in the monomer feed. This is related to the

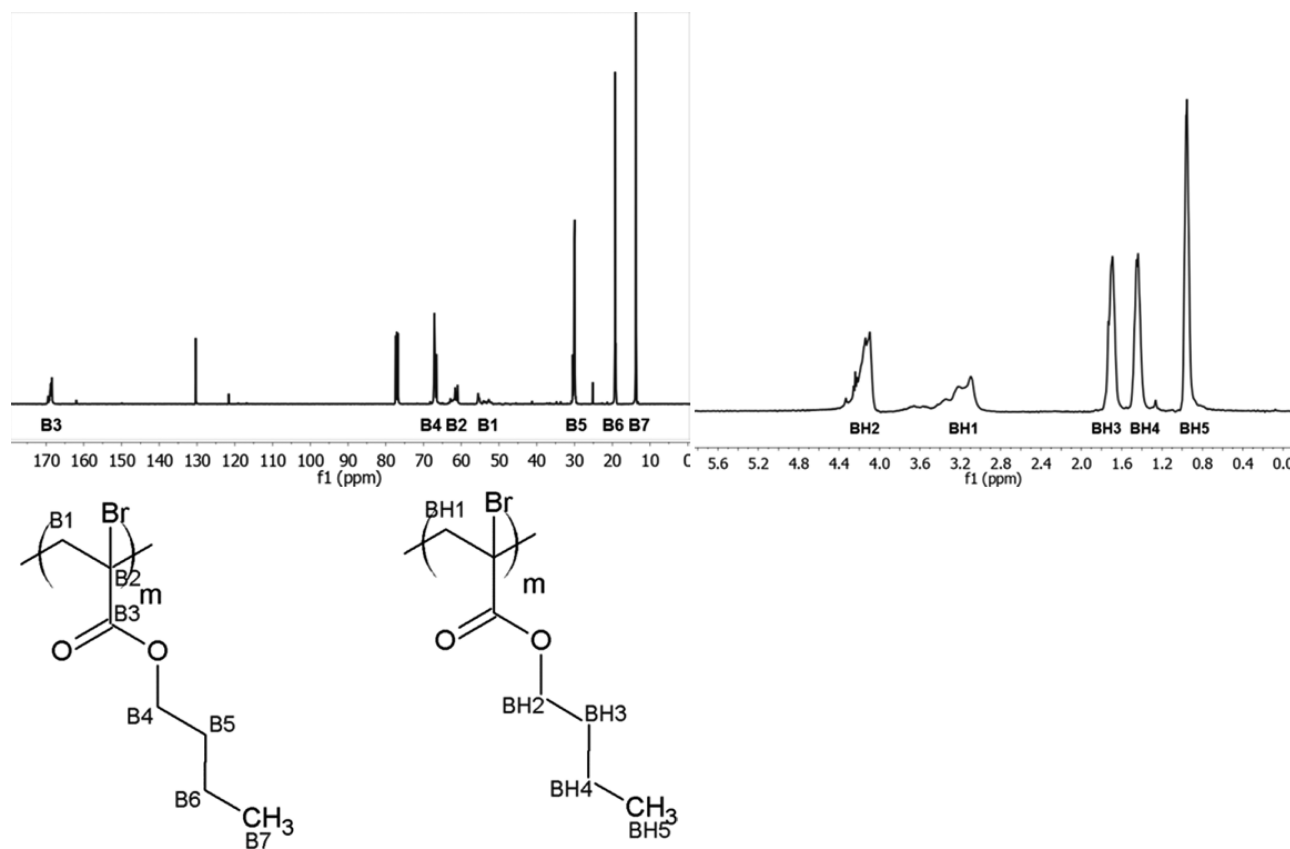


Figure 2. ^{13}C and ^1H NMR spectra of poly(butyl 2-bromoacrylate) and the assigned structure.

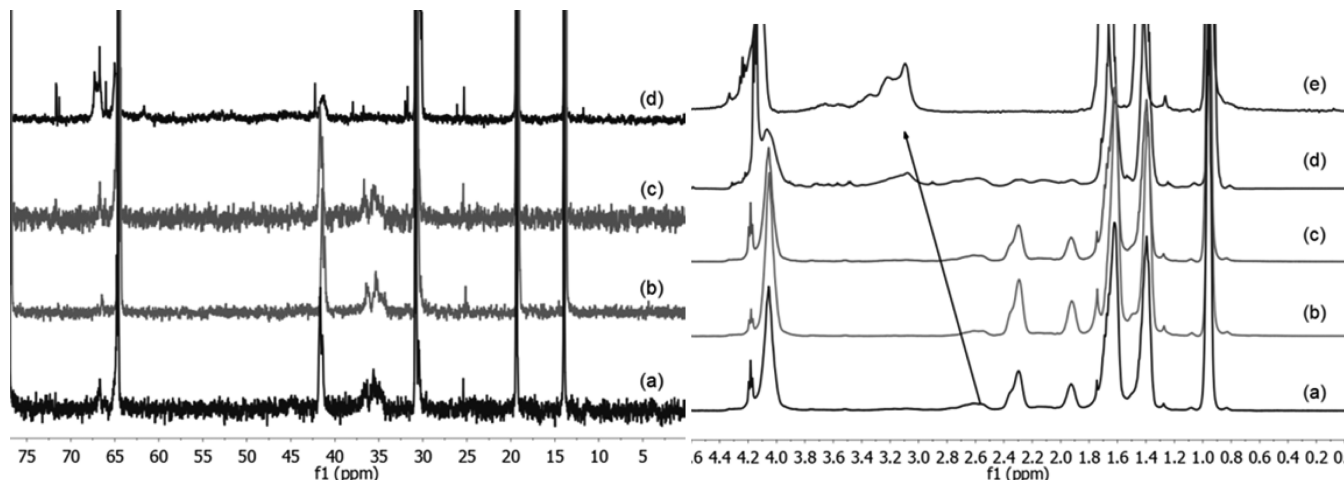


Figure 3. Nonquantitative ^{13}C and ^1H NMR spectra of poly(butyl acrylate-*co*-butyl 2-bromoacrylate) at varying concentrations: (a) 5, (b) 10, (c) 20, (d) 50, and (e) 100 wt % (^1H NMR only) of butyl 2-bromoacrylate in comonomer feed.

change in the triad distribution upon changing the monomer feed composition, resulting in substantial broadening of the peak in addition to large chemical shift.

We proceeded to check the limit of detection of the patched bromide structure by copolymerizing low amounts of the bromomonomer and performing quantitative carbon NMR experiments. The majority of signals that are attributed to the midchain bromide structure overlap with that of butyl acrylate due to its structural similarity, particularly for carbons some distance away from the bromide atom such as the methylene groups in the butyl unit. It is very difficult to quantify the amount of the quaternary carbon arising from the midchain bromide because although it is shifted significantly from the quaternary carbon of poly(butyl acrylate), the peak is so broad that at low concentrations the signal-to-noise ratio does not provide sufficient information to yield even qualitative information. The peak arising from the carbonyl group next to the bromide (peak B3 in Figure 2) is sharp enough to yield information, but it overlaps with the carbonyl at the polymer end group with bromide attached (labeled I4 in Figure 1) and is of little use for quantification in the ATRP reaction where the concentration of this species should be high (see Figure S7).

The most useful signal for quantification of the midchain bromide arises from the signal related to the OCH_2 carbon attached to the midchain bromide quaternary carbon at 66.4 ppm. Figure 4 shows this region and demonstrates that even with contents as low as 0.8 mol % it is possible to observe the structure of the patched tertiary radical. The signal can clearly be distinguished from both the structurally similar carbons related to the main part of the butyl acrylate polymer chain at 64.2 ppm and to the bromide end group unit at 65.6 ppm. In addition, integration of these peaks yields good agreement with the amount of the bromide containing monomer in the monomer feed, giving 3.0 and 1.2 mol % for monomer feeds of 3.2 and 0.8 mol %, respectively.

The spectra of the ATRP sample do not show any signal in this region. However, the ATRP led to a decrease in the fraction of C_q of 2 mol % compared to free radical polymerization (see Table 1). If the irreversible deactivation of the midchain radical were the cause for this decrease, the concentration of the midchain bromide would be around 2%, which is well within the range of detection shown here. Therefore, it can be concluded that the patched midchain

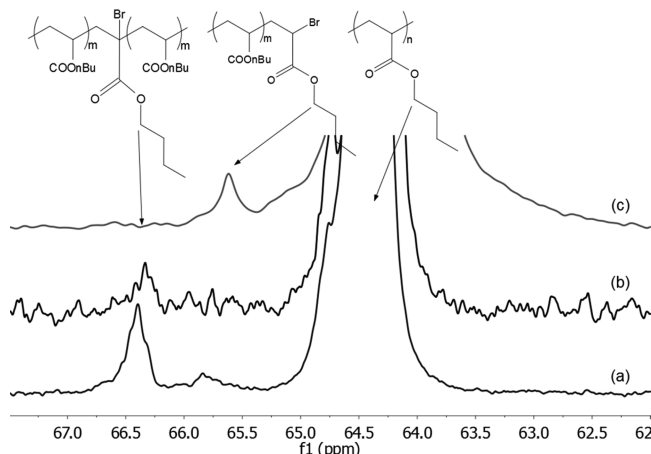
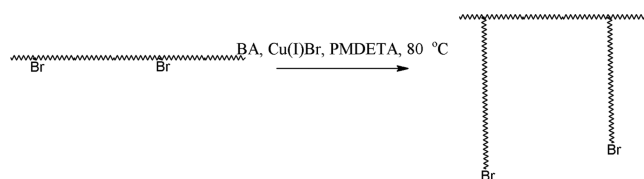


Figure 4. ^{13}C NMR spectra showing the appearance of peaks relating to the OCH_2 carbon for sample of (a) poly(butyl acrylate-*co*-butyl 2-bromoacrylate) with 3.2 mol % butyl 2-bromoacrylate in the monomer feed, (b) poly(butyl acrylate-*co*-butyl 2-bromoacrylate) with 0.8 mol % butyl 2-bromoacrylate in the monomer feed, and (c) poly(butyl acrylate) synthesized by ATRP. The spectra have been normalized by the peak of highest intensity in the spectra so peak integrals in the figure are qualitatively comparable.

bromide structure is not the reason for the reduction in branching in ATRP reactions.

In order to further prove that tertiary radical capping is not the cause of reduced branching, we performed a chain extension of a poly(butyl acrylate-*co*-butyl 2-bromoacrylate) macroinitiator by ATRP (see Scheme 5). If the effect of the ATRP equilibrium favoring formation of the midchain bromide over propagation of the tertiary radical species were indeed the

Scheme 5. Chain Extension by ATRP Using Poly(butyl acrylate-*co*-butyl 2-bromoacrylate) Macroinitiator



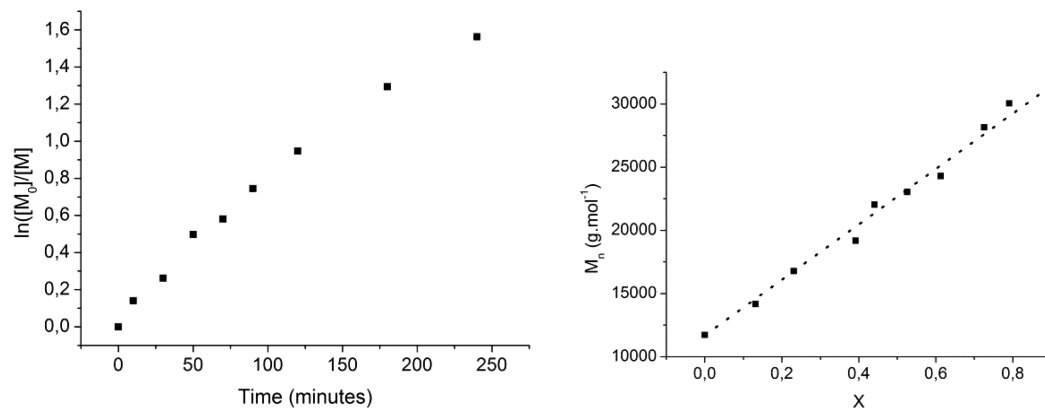


Figure 5. First-order kinetic plot and evolution of molecular weight with conversion (dashed line represents the theoretical increase).

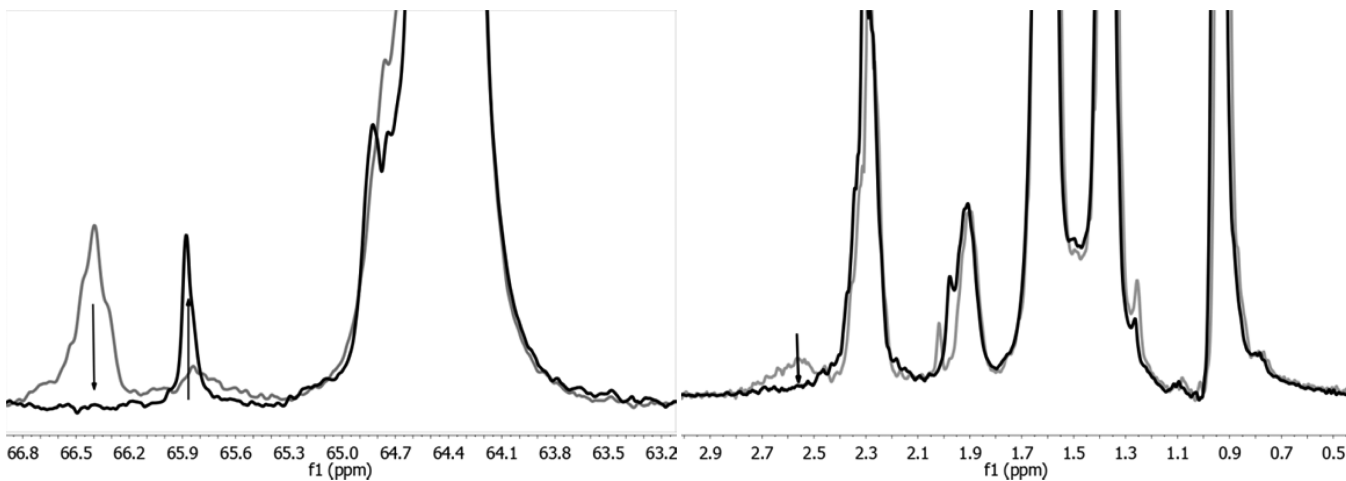


Figure 6. ^{13}C and ^1H NMR spectra in the regions of interest for poly(butyl acrylate-*co*-butyl 2-bromoacrylate) macroinitiator (gray) and the polymer produced by chain extension of the macroinitiator by ATRP (black).

cause of reduced branching in ATRP, then it would be expected that such a reaction would show slow initiation and maintain a high level of the midchain bromide throughout the reaction.

The multifunctional macroinitiator was synthesized by bulk copolymerization of butyl acrylate and butyl 2-bromoacrylate (95:5 weight ratio) in the presence of octylthiol to obtain a moderate molecular weight copolymer, and the reaction was terminated at 85% conversion. The reactivity ratios of butyl acrylate and butyl 2-bromoacrylate were calculated by low conversion copolymer composition experiments and were shown to be $r_{\text{BrBA}} = 9.77$ and $r_{\text{BA}} = 0.24$ (see Figures S13 and S14). The high reactivity ratio for butyl 2-bromoacrylate thus results in some composition drift, and the average number of bromides per polymer chain varies between 12 and 0 throughout the polymerization with a monomer feed of 97 mol % butyl acrylate and assuming a constant degree of polymerization of 90 (corresponding to the experimentally determined M_n value) throughout the polymerization (see Figure S15). The macroinitiator had low branching fraction (0.2 mol % calculated from ^{13}C NMR spectra) as may be expected due to a combination of lower reaction temperature, presence of chain transfer agent,^{21,31,32} and the comonomer which may inhibit the formation of the tertiary radical.^{51,52}

The copolymer was used as macroinitiator in an ATRP reaction to form a branched polymer. The evolution of conversion and molecular weight with time is shown in Figure 5. It is clear from this that the reaction proceeds without any

inhibitory effects arising from slow initiation from the midchain bromide that could be expected if the reason for reduced branching in ATRP is the equilibrium kinetics preventing propagation from the tertiary radical. In addition, the molecular weight increased linearly with conversion matching well with the theoretical increase in molar mass calculated from

$$M_{n,\text{theo}} = M_n^0 + M_{\text{BA}} X n_{\text{BrBA}} \frac{[\text{BA}]}{[\text{I}]}$$

where M_n^0 is the molecular weight of the macroinitiator, M_{BA} is the molar mass of butyl acrylate, X is the conversion, and n_{BrBA} is the average number of butyl 2-bromoacrylate units per macroinitiator chain calculated from dividing M_n^0 by M_{BA} to give the number-average degree of polymerization and multiplying by the mole fraction of butyl 2-bromoacrylate in the copolymer (3 mol %). The PDI remained around 2 throughout due to the polydispersity of the macroinitiator which was produced by conventional free radical polymerization. It can be expected, based on the assumption that the amount of bromide per unit length in the macroinitiator is constant, that the evolution of molecular weight with conversion follows this linear form if initiation is rapid and that no significant broadening of the molecular weight distribution will occur. Analysis of the molecular weight distribution (Figure S16) shows that there are no low molecular weight polymers being formed and confirms that growth of polymer chains occurs solely from the

tertiary radical formed by activation of the midchain bromide. In addition, there is no lower molecular weight tail that may arise from slow initiation from the tertiary center, nor a high molecular weight shoulder that may arise from excessive radical coupling.

The ^1H and ^{13}C NMR confirm the loss of the midchain bromide. Figure 6 shows the regions of interest of the NMR spectra of the macroinitiator and the polymer obtained after the ATRP reaction. In the ^1H NMR the signal from the CH_2 hydrogens in the backbone next to the bromide disappears while the ^{13}C NMR shows a complete disappearance of the strong signal arising from the OCH_2 carbon next to the midchain bromide and a corresponding increase in the signal due to the OCH_2 of the end chain bromide capped secondary radical.

In addition, the C_q carbon increased in intensity from 0.2 mol % in the macroinitiator to 1.2 mol % in the chain-extended polymer. This large increase can be attributed to the production of branching points from the midchain bromide used as initiating moiety. Figure 7 shows the increase in the intensity of

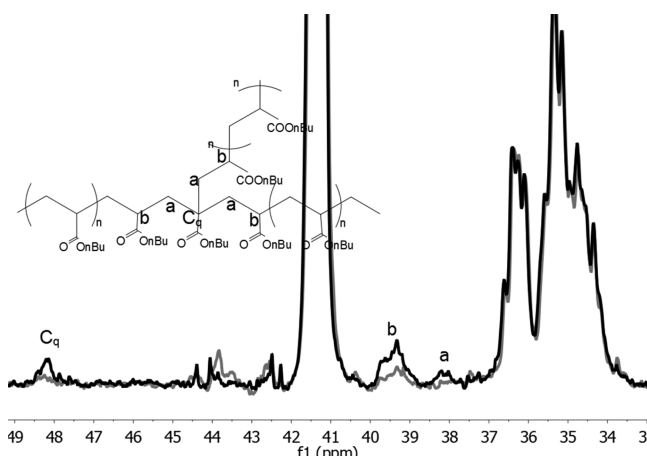


Figure 7. ^{13}C for poly(butyl acrylate-*co*-butyl 2-bromoacrylate) macroinitiator (gray) and the polymer produced by chain extension of the macroinitiator by ATRP (black).

the signals resulting from the quaternary carbon formed after chain extension by ATRP. The increase in quaternary carbon corresponds well to the theoretical increase assuming that all midchain bromides act as an initiating site to create a branch point. The evidence that initiation from the midchain bromide in ATRP is fast and that the midchain bromide is efficiently consumed during the polymerization further confirms that the

irreversible trapping of the tertiary radical is not the cause for reduction of branching in ATRP.

Finally, we performed *ab initio* calculations to determine the free energy change upon formation of the secondary and tertiary radicals in the ATRP reaction to observe whether the argument for the ATRP equilibria being responsible for the reduction in branching can be upheld theoretically. The results for the energy levels are shown in Figure 8 and show that the tertiary radical is energetically more stable, and combined with the known effect of secondary versus tertiary radicals for small molecule ATRP initiators (K_{ATRP} of methyl bromopropionate is nearly 2 orders of magnitude less than that of methyl bromoisobutyrate)⁵³ it would seem reasonable to assume a significantly higher equilibrium constant for the tertiary radical. This would lead to a high concentration of the radical and therefore relatively high rates of propagation that would seem to further reinforce the idea that patching of the tertiary radical by a bromide is not the cause of the reduction in branching in ATRP polymerizations.

CONCLUSIONS

In conclusion, we have shown that the reduction in branching in ATRP of butyl acrylate is not caused by patching of the midchain radical with a bromide atom. By synthesis of a copolymer of poly(butyl acrylate-*co*-butyl 2-bromoacrylate) we have shown the midchain bromide can be quantified at low concentrations by ^{13}C NMR, and it was not found in samples synthesized by ATRP. In addition, it is shown that a poly(butyl acrylate-*co*-butyl 2-bromoacrylate) can be used as macroinitiator in ATRP which indicates that the bromide-capped midchain radical is efficiently activated. This result demonstrates that tertiary radical capping is not irreversible in ATRP and is not the cause of reduced branching compared to conventional radical polymerization. This conclusion is further supported by *ab initio* calculations that demonstrate the midchain tertiary radical has increased stability compared to the secondary radical.

ASSOCIATED CONTENT

Supporting Information

Complete molecular weight distributions, 2D NMR spectra of polymers, reactivity ratio experiments, and NMR spectra of monomers. This material is available free of charge via the Internet at <http://pubs.acs.org>.

AUTHOR INFORMATION

Corresponding Author

*E-mail jm.asua@ehu.es (J.M.A.).

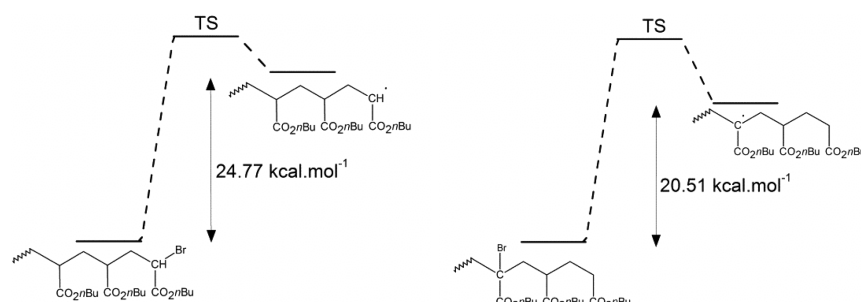


Figure 8. Energy levels of the secondary and tertiary radicals compared to the bromide-capped species calculated by *ab initio* methods.

Notes

The authors declare no competing financial interest.

ACKNOWLEDGMENTS

Diputación Foral de Gipuzkoa, University of Basque Country (UFI 11/56), Basque Government (GVIT373-10 and Etortek Nanoiker IE11-304), and Ministerio de Economía y Competitividad (CTQ2011-25572) are gratefully acknowledged for their financial support. The SGI/IZO-SGIker UPV/EHU is gratefully acknowledged for generous allocation of computational resources.

REFERENCES

- (1) Plessis, C.; Arzamendi, G.; Leiza, J. R.; Schoonbrood, H. A. S.; Charmot, D.; Asua, J. M. *Macromolecules* **2000**, *33*, 4–7.
- (2) Plessis, C.; Arzamendi, G.; Leiza, J. R.; Schoonbrood, H. A. S.; Charmot, D.; Asua, J. M. *Macromolecules* **2000**, *33*, 5041–5047.
- (3) Plessis, C.; Arzamendi, G.; Alberdi, J. M.; Agnely, M.; Leiza, J. R.; Asua, J. M. *Macromolecules* **2001**, *34*, 6138–6143.
- (4) Nikitin, A. N.; Castignolles, P.; Charleux, B.; Vairon, J.-P. *Macromol. Rapid Commun.* **2003**, *24*, 778–782.
- (5) Plessis, C.; Arzamendi, G.; Alberdi, J. M.; van Herk, A. M.; Leiza, J. R.; Asua, J. M. *Macromol. Rapid Commun.* **2003**, *24*, 173–177.
- (6) Willemse, R. X. E.; van Herk, A. M.; Panchenko, E.; Junkers, T.; Buback, M. *Macromolecules* **2005**, *38*, 5098–5103.
- (7) Nikitin, A. N.; Hutchinson, R. A. *Macromolecules* **2005**, *38*, 1581–1590.
- (8) Chauvet, J.; Asua, J. M.; Leiza, J. R. *Polymer* **2005**, *46*, 9555–9561.
- (9) Junkers, T.; Schneider-Baumann, M.; Koo, S. S. P.; Castignolles, P.; Barner-Kowollik, C. *Macromolecules* **2010**, *43*, 10427–10434.
- (10) Agirre, A.; Nase, J.; Degrandi, E.; Creton, C.; Asua, J. M. *Macromolecules* **2010**, *43*, 8924–8932.
- (11) Qie, L.; Dubé, M. A. *J. Appl. Polym. Sci.* **2012**, *124*, 349–364.
- (12) Reyes, Y.; Arzamendi, G.; Asua, J. M.; Leiza, J. R. *Macromolecules* **2011**, *44*, 3674–3679.
- (13) Junkers, T.; Barner-Kowollik, C. *J. Polym. Sci., Part A: Polym. Chem.* **2008**, *46*, 7585–7605.
- (14) González, I.; Leiza, R.; Asua, M. *Macromolecules* **2006**, *39*, 5015–5020.
- (15) Yu-Su, S. Y.; Sun, F. C.; Sheiko, S. S.; Konkolewicz, D.; Lee, H.; Matyjaszewski, K. *Macromolecules* **2011**, *44*, 5928–5936.
- (16) Farcet, C.; Belleney, J.; Charleux, B.; Pirri, R. *Macromolecules* **2002**, *35*, 4912–4918.
- (17) Yu, X.; Broadbelt, L. J. *Macromol. Theory Simul.* **2012**, *21*, 461–469.
- (18) Cuccato, D.; Mavrouidakis, E.; Dossi, M.; Moscatelli, D. *Macromol. Theory Simul.* **2013**, *22*, 127–135.
- (19) Sato, E.; Emoto, T.; Zetterlund, P. B.; Yamada, B. *Macromol. Chem. Phys.* **2004**, *205*, 1829–1839.
- (20) Yamada, B.; Azukizawa, M.; Yamazoe, H.; Hill, D. J.; Pomery, P. *Polymer* **2000**, *41*, 5611–5618.
- (21) Junkers, T.; Koo, S. P. S.; Davis, T. P.; Stenzel, M. H.; Barner-Kowollik, C. *Macromolecules* **2007**, *40*, 8906–8912.
- (22) Koo, S. P. S.; Junkers, T.; Barner-Kowollik, C. *Macromolecules* **2009**, *42*, 62–69.
- (23) Buback, M.; Hesse, P.; Junkers, T.; Sergeeva, T.; Theis, T. *Macromolecules* **2008**, *41*, 288–291.
- (24) Britton, D.; Heatley, F.; Lovell, P. A. *Macromolecules* **1998**, *31*, 2828–2837.
- (25) Heatley, F.; Lovell, P. A.; Yamashita, T. *Macromolecules* **2001**, *34*, 7636–7641.
- (26) Ahmad, N. M.; Heatley, F.; Lovell, P. A. *Macromolecules* **1998**, *31*, 2822–2827.
- (27) Castignolles, P.; Graf, R.; Parkinson, M.; Wilhelm, M.; Gaborieau, M. *Polymer* **2009**, *50*, 2373–2383.
- (28) Asua, J. M.; Beuermann, S.; Buback, M.; Castignolles, P.; Charleux, B.; Gilbert, R. G.; Hutchinson, R. A.; Leiza, J. R.; Nikitin, A. N.; Vairon, J.-P.; van Herk, A. M. *Macromol. Chem. Phys.* **2004**, *205*, 2151–2160.
- (29) Liang, K.; Hutchinson, R. A.; Barth, J.; Samrock, S.; Buback, M. *Macromolecules* **2011**, *44*, 5843–5845.
- (30) Liang, K.; Hutchinson, R. A. *Macromol. Rapid Commun.* **2011**, *32*, 1090–S.
- (31) Gaborieau, M.; Koo, S. P. S.; Castignolles, P.; Junkers, T.; Barner-Kowollik, C. *Macromolecules* **2010**, *43*, 5492–5495.
- (32) Agirre, A.; Santos, J. I.; Etxeberria, A.; Sauerland, V.; Leiza, J. R. *Polym. Chem.* **2013**, *4*, 2062–2079.
- (33) Barner-Kowollik, C.; Günzler, F.; Junkers, T. *Macromolecules* **2008**, *41*, 8971–8973.
- (34) Ahmad, N. M.; Charleux, B.; Faracet, C.; Ferguson, C. J.; Gaynor, S. G.; Hawkett, B. S.; Heatley, F.; Klumperman, B.; Konkolewicz, D.; Lovell, P. A.; Matyjaszewski, K.; Venkatesh, R. *Macromol. Rapid Commun.* **2009**, *30*, 2002–21.
- (35) Reyes, Y.; Asua, J. M. *Macromol. Rapid Commun.* **2011**, *32*, 63–67.
- (36) Konkolewicz, D.; Sosnowski, S.; D'hooge, D. R.; Szymanski, R.; Reyniers, M.-F.; Marin, G. B.; Matyjaszewski, K. *Macromolecules* **2011**, *44*, 8361–8373.
- (37) Strazielle, C.; Benoit, H.; Vogl, O. *Eur. Polym. J.* **1978**, *14*, 331–334.
- (38) Penzel, E.; Goetz, N. *Angew. Makromol. Chem.* **1990**, *178*, 191–200.
- (39) Haddleton, D. M.; Crossman, M. C.; Dana, B. H.; Duncalf, D. J.; Heming, A. M.; Kukulj, D.; Shooter, A. J. *Macromolecules* **1999**, *32*, 2110–2119.
- (40) Cartwright, D.; Turnbull, M. A Process for Preparing 2-pyridinyloxyphenoxy-lower-alkanoates. U.S. Patent 4,414,391, Nov 8 1983.
- (41) van Herk, A. M.; van Droege, T. *Macromol. Theory Simul.* **1997**, *12*, 1263–1276.
- (42) Frisch, M. J.; Trucks, G. W.; Schlegel, H. B.; Scuseria, G. E.; Robb, M. A.; Cheeseman, J. R.; Scalmani, G.; Barone, V.; Mennucci, B.; Petersson, G. A.; Nakatsuji, H.; Caricato, M.; Li, X.; Hratchian, H. P.; Izmaylov, A. F.; Bloino, J.; Zheng, G.; Sonnenberg, J. L.; M. Had, D. J. F. Gaussian 9, Revision A.1; Gaussian Inc.: Wallingford, CT, 2009.
- (43) Zhao, Y.; Truhlar, D. G. *Theor. Chem. Acc.* **2008**, *120*, 215.
- (44) Dunning, T. H. *J. Chem. Phys.* **1989**, *90*, 1007.
- (45) Wilson, A. K.; Woon, D.; Peterson, K. A.; Dunning, T. H. *J. Chem. Phys.* **1999**, *110*, 7667.
- (46) Balabanov, N. B.; Peterson, K. A. *J. Chem. Phys.* **2005**, *123*, 064107.
- (47) Cancès, E.; Mennucci, B.; Tomasi, J. *J. Chem. Phys.* **1997**, *107*, 3032.
- (48) Barone, V.; Cossi, M.; Tomasi, J. *J. Comput. Chem.* **1998**, *19*, 404.
- (49) Barone, V.; Cossi, M.; Tomasi, J. *J. Chem. Phys.* **1997**, *107*, 3210.
- (50) Cossi, M.; Barone, V.; Cammi, R.; Tomasi, J. *J. Chem. Phys. Lett.* **1996**, *255*, 327.
- (51) González, I.; Asua, J. M.; Leiza, J. R. *Polymer* **2007**, *48*, 2542–2547.
- (52) Plessis, C.; Arzamendi, G.; Leiza, J. R.; Schoonbrood, H. A. S.; Charmot, D.; Asua, M.; Sebastia, E. D. *Macromolecules* **2001**, *34*, 5147–5157.
- (53) Tang, W.; Kwak, Y.; Braunecker, W.; Tsarevsky, N. V.; Coote, M. L.; Matyjaszewski, K. *J. Am. Chem. Soc.* **2008**, *130*, 10702–10713.